

Supporting Information for

Absorption and Quantum Yield of Single Conjugated Polymer Poly[2-methoxy-5-(2-ethylhexyloxy)-1,4-phenylenevinylene] (MEH-PPV) Molecules

Lei Hou*, Subhasis Adhikari*, Yuxi Tian[†], Ivan G. Scheblykin⁺, Michel Orrit*

Corresponding: orrit@physics.leidenuniv.nl

* LION, Huygens-Kamerlingh Onnes Laboratory, Leiden University

Niels Bohrweg 2, 2300RA Leiden, the Netherlands

⁺ Chemical Physics and Nano Lund, Lund University, PO Box 124, 22100, Lund, Sweden

[†] Key Laboratory of Mesoscopic Chemistry of MOE and School of Chemistry and Chemical Engineering, Nanjing University, 210023 Nanjing, China

1. Experimental setup and calibration of photothermal signals using gold nanoparticles;
2. Collection efficiency of the optical setup;
3. Excitation power dependence of the fluorescence and the photothermal signal of MEH-PPV films;
4. Fluorescence spectrum of single MEH-PPV polymers under study;
5. Decay of fluorescence and absorption with illumination time;

6. Calibration factor in the evaluation of the absorption cross section of single molecules;
7. Blinking time traces of single MEH-PPV molecules dispersed in PMMA by direct spin casting from toluene;
8. Schematic representation of an extended conformation of a MEH-PPV chain with some collapsed regions;
9. Continuous photo-bleaching traces with small intermittent steps;
10. Effect of xenon pressure on the photophysics of MEH-PPV molecules.

1. Experimental setup and calibration of photothermal signals using gold nanoparticles.

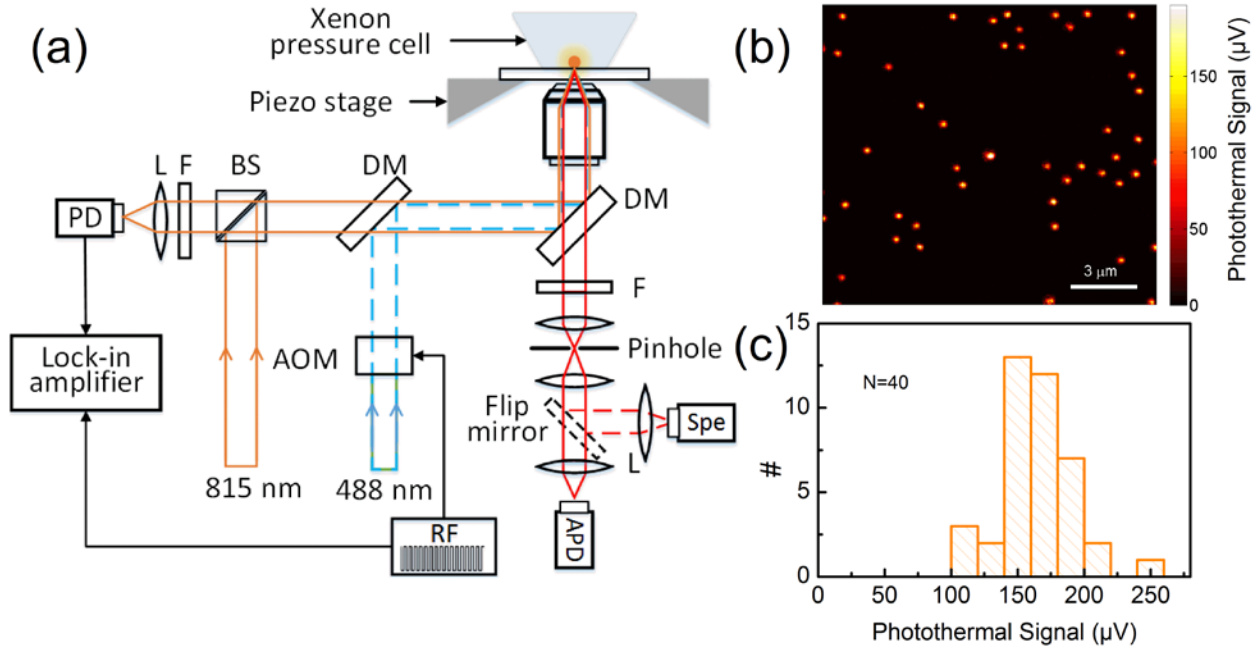


Figure S1: Experimental setup and calibration of photothermal signal with 20 nm gold nanoparticles in near-critical xenon. (a) A scheme of the experimental setup. DM: dichroic mirror; AOM: acoustic-optical modulator; BS: beam splitter; RF: radio-frequency signal generator; PD: photodiode; F: optical filter; L: lens; Spe: spectrometer; APD: Avalanche photodiode. (b) Typical photothermal confocal image of 20 nm gold spheres on glass and imbedded in PMMA matrix in near-critical xenon when the temperature and pressure are close to the optimal conditions (288 K and 6.26 MPa in this case). (c) Histogram of the photothermal signals of 40 particles in (b).

2. Collection efficiency of the optical setup.

We estimate the detection efficiency of our optical setup using 20 nm gold spheres in glycerol. From a previous study, the one-photon photoluminescence quantum yield of a 20 nm gold particle in glycerol was measured to be about

3.7×10^{-7} , using 514 nm laser as excitation [1]. Even though the photoluminescence quantum yield of single gold nanoparticles might depend on the excitation wavelength [2], we do not expect too much difference in quantum yield when we use a 488 nm laser for excitation, because the two wavelengths are close to each other, and both photon energies are higher than the energy of interband transitions of gold. So we use 3.7×10^{-7} as the quantum yield of single 20 nm gold spheres to estimate the detection efficiency of the setup, considering all the factors including the collection efficiency of the objective, the transmission loss of all the optics in the fluorescence detection path, confocal pinhole and the quantum efficiency of the APD photo-detector.

We use about 65.8 kW/cm^2 excitation intensity at 488 nm to image the photoluminescence of single 20 nm gold spheres in glycerol. We fit the spots in the image with 2D Gaussian functions, and extract the intensity of these particles. The mean photoluminescence intensity over 8 particles is about 22,700 counts/s. From the excitation power and photothermal signal, we can get the number of photons absorbed by the gold nanoparticle, about 4.7×10^{11} photons/s. Considering the quantum yield mentioned above, we get a collection efficiency of our optical setup of about 0.13.

3. Excitation power dependence of the fluorescence and the photothermal signal of MEH-PPV films.

In order to estimate the excitation power range where the photothermal signal and the fluorescence signal are in the linear regime, we measured the power dependence of those two signals with thin MEH-PPV films. A concentrated solution of MEH-PPV in chloroform (0.66 mg/L) was spin-coated on a clean cover glass and covered with a PMMA layer. The pressure and temperature of the sample cell are 6.2 MPa and 288 K. The estimated temperature rise in the focal volume is less than 1 K. The power dependence curve is shown in Fig.S2. We can see that the fluorescence and photothermal signals well follow the linear relationship with excitation power when the power is below 500 W/cm^2 .

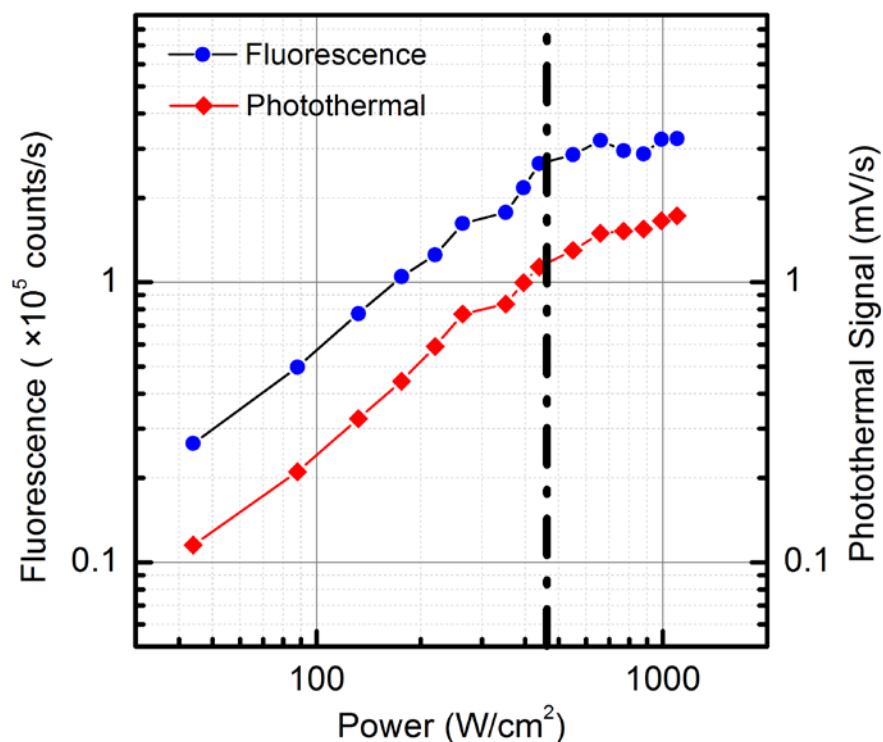


Figure S2: Excitation power dependence of the fluorescence and the photothermal signals of the MEH-PPV film. The dashed-dot line indicates the power used in the single-molecule measurements.

4. Fluorescence spectrum of single MEH-PPV polymer under study.

The single conjugated polymers consist of many chromophores, and there is no widely accepted criterion to identify such multi-chromophore systems as single polymer chains. In our experiments, we use different ways to confirm the single polymer chains. First, the deduced number of monomers in each chain matches what is expected for the sample we used; Second, we measured the emission spectra of the emitting spots, and a typical spectrum is shown in Fig. S3. The spectrum is broadly distributed around 580 nm, which resembles the results in refs. [3, 4]. When we record the spectrum as a function of illumination time, we did not find much change in the peak position and shape, only a decrease of the total intensity. This result is in accordance with continuous bleaching, where the photophysics is dominated by conjugated polymer chains with

extended conformations, and many independent segments in a chain with limited energy transfer contribute to the emission.

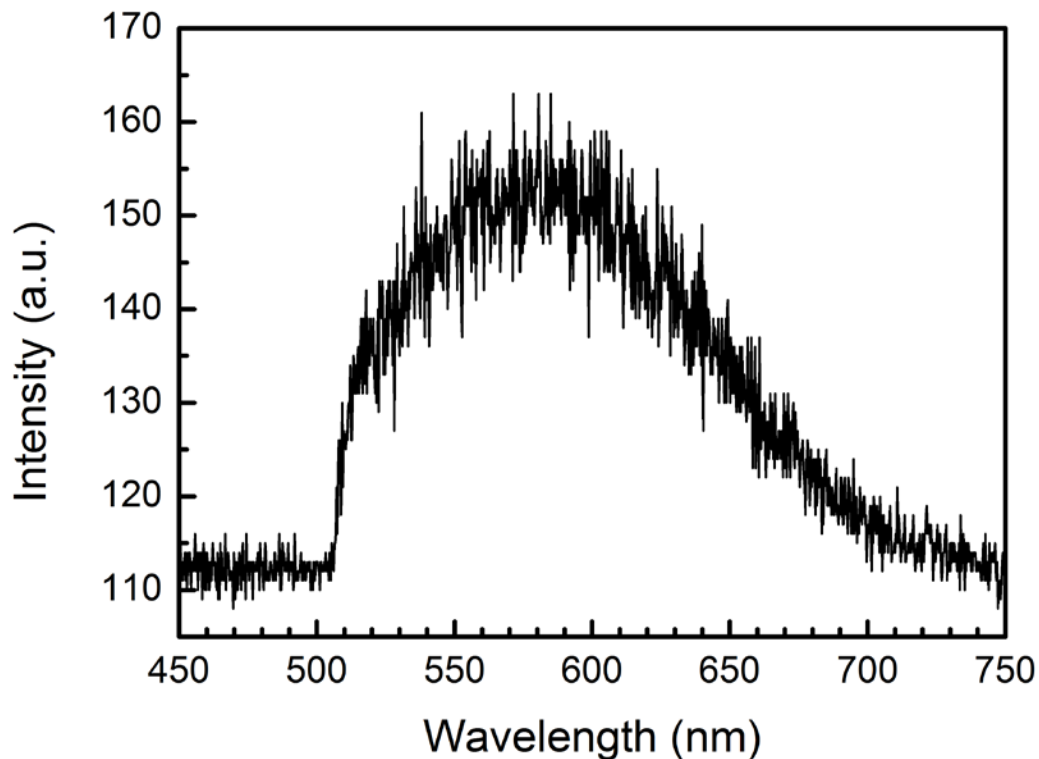


Figure S3: A typical fluorescence spectrum of a single MEH-PPV polymer molecule. The sample in this measurement is the same as the one used in the main text. The excitation power is about 450 W/cm^2 at 488 nm ; the integration time is 1 s . Long-pass filters are used to remove the excitation, as shown by the cut-off edge around 510 nm .

5. Decay of fluorescence and absorption with illumination time.

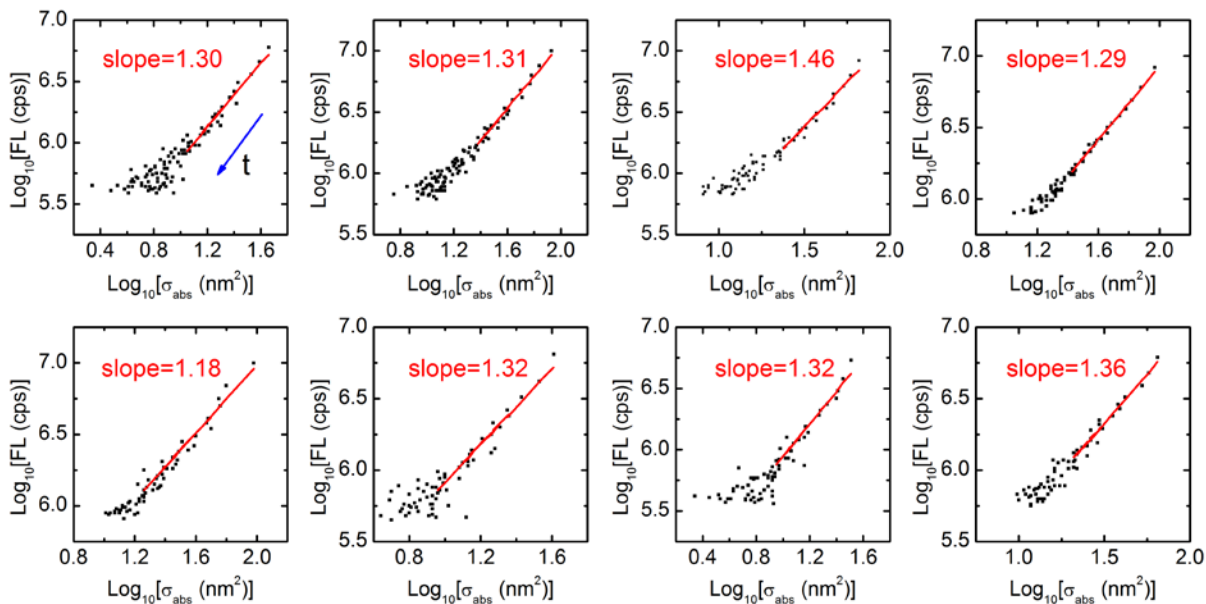


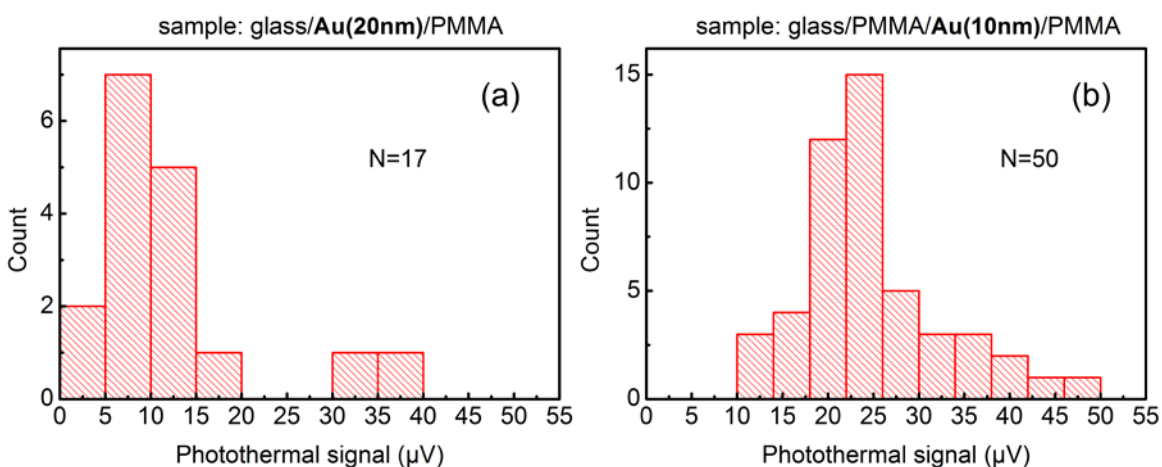
Figure S4: Correlated decays of fluorescence and absorption of eight single MEH-PPV molecules with the illumination time. 10 points in the raw time traces were binned into one point shown in each plot. The blue arrow indicates the time evolution. Most cases show a clear super-linear behavior, with slope larger than unity.

6. Calibration factor in the evaluation of the absorption cross section of single molecules.

Contrary to the single-molecule polymer experiments, the gold nanoparticle sample used to calibrate the photothermal signal did not have the lower PMMA layer close to the cover glass to form the sandwich structure. To correct for this difference, we additionally measured the photothermal signal of 20 nm and 10 nm gold nanoparticles with and without the PMMA layer in near-critical xenon. These two pairs of measurements were necessary because they were done at different times, with possibly slightly different adjustments of the photothermal microscope.

For the sample with a glass/PMMA/**10nm Au**/PMMA structure, with 17.6 μW heating power and 0.7 mW probe power at the sample, 10 ms integration time, 6.2 MPa pressure and 15.2 $^{\circ}\text{C}$ temperature in the xenon cell, the average photothermal signal over 50 particles is $21.7 \pm 7.7 \mu\text{V}$; For the sample with a glass/**20nm Au**/PMMA structure, under the same conditions as above, except the heating power 4.4 μW at the sample, the average photothermal signal over 17 particles is $12.7 \pm 8.6 \mu\text{V}$. The photothermal signal of single gold nanoparticles goes linearly with the heating power, as shown Fig.S5 (c). Thus, the average photothermal signal of those **20 nm** nanoparticles with a glass/Au/PMMA structure at 17.6 μW heating power is about 50.8 μV . Since the absorption cross section of gold nanospheres scales with the third power of radius (R^3), the photothermal signal (which scales with the absorption cross section) of **10 nm** gold nanoparticle in a glass/Au/PMMA structure is expected to be **6.35 μV** under 17.6 μW heating power.

Then the correction factor of photothermal signal due to the presence of a PMMA layer on the glass is $21.7/6.35 = \mathbf{3.4}$. This factor was considered when the photothermal signal of single MEH-PPV molecules was converted into the absorption cross section.



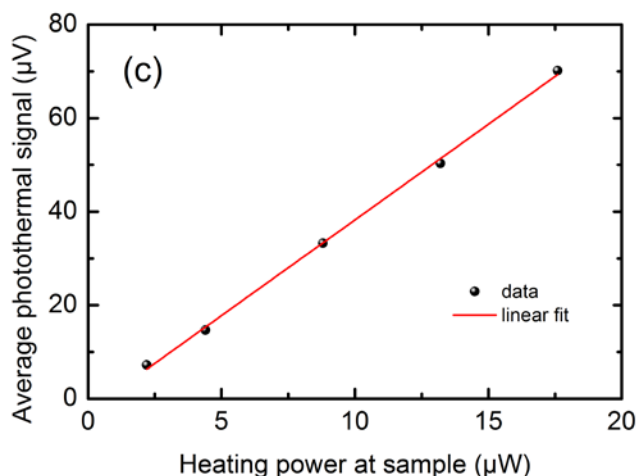


Figure S5: Histogram of photothermal signals with (a): a glass/20nm Au/PMMA structure; (b): a glass/PMMA/10nm Au/PMMA structure. (c) Power dependence of the photothermal signal with the glass/20nm Au/PMMA structure sample.

7. Blinking time traces of single MEH-PPV molecules dispersed in PMMA by direct spin casting from toluene.

When we spin-coated a MEH-PPV and PMMA mixture in toluene on a glass and measured the time trace of single molecules, we could observe the blinking fluorescence transients shown below. The photothermal signal was too weak to be measurable in this case. Spin-coating a chloroform solution of MEH-PPV, however, leads mostly to continuously bleaching spots as shown in the main text (see Fig.4 in main text).

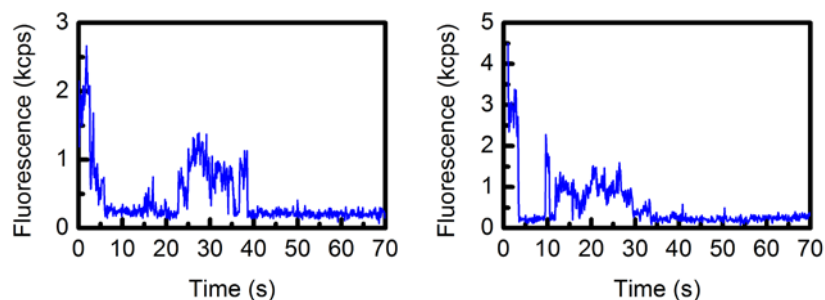


Figure S6: Blinking time traces of two MEH-PPV molecules prepared by spin-coating a MEH-PPV and PMMA mixture in toluene on a glass slide.

8. Schematic representation of an extended conformation of a MEH-PPV chain with some collapsed regions.

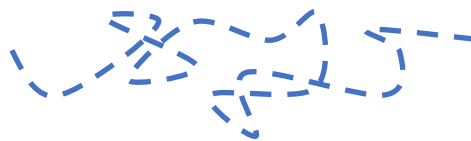


Figure S7: A schematic representation of an extended MEH-PPV chain with some collapsed regions (kinks and knots) in it.

9. Continuous photo-bleaching traces with small intermittent steps.

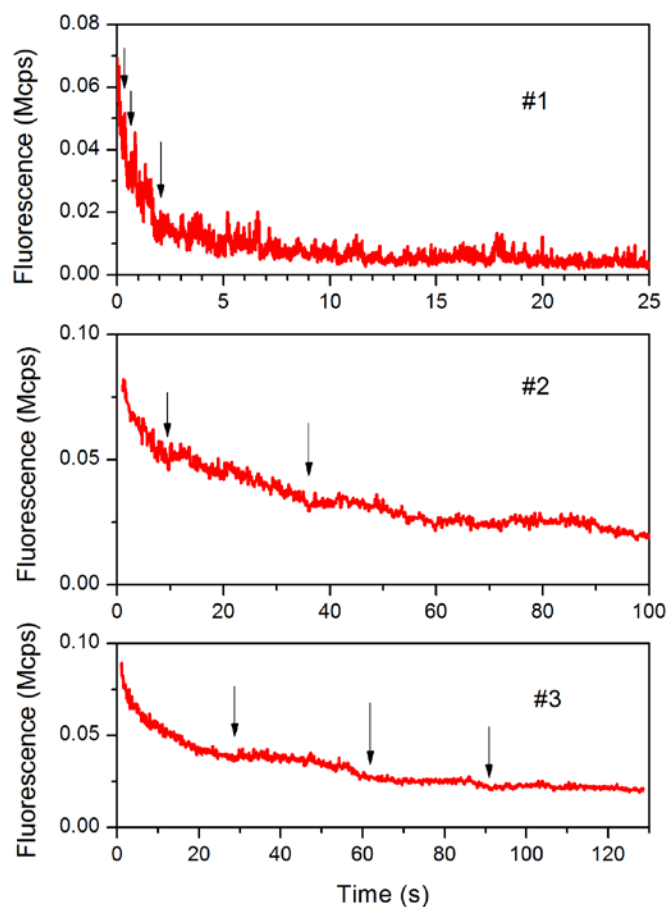


Figure S8: Continuous photo-bleaching traces of three MEH-PPV molecules with small steps marked with black arrows that could arise from intermittency or blinking of parts of the molecule. The sample preparation is the same as for the main text.

10. Effect of xenon pressure on the photophysics of MEH-PPV molecules.

We measured the same sample as used in the main text at low xenon pressure to see if high pressure xenon has some effects on the photophysics of the MEH-PPV molecules. We obtained similar results in the fluorescence signal as shown in Fig.S9. The photothermal signal was not measurable at low xenon pressure.

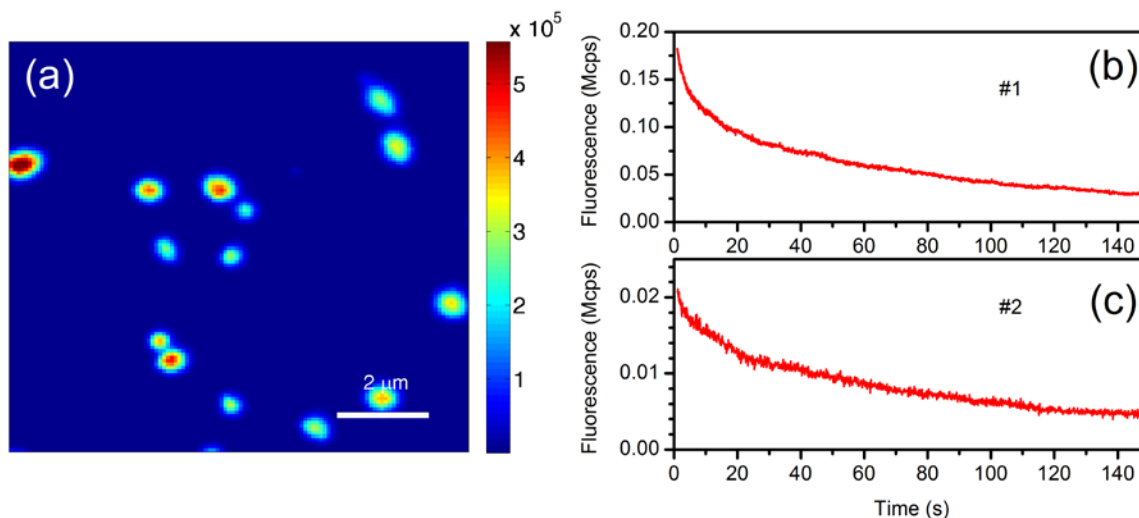


Figure S9: (a) Fluorescence of MEH-PPV molecules at low xenon pressure. The excitation power is about 45 W/cm^2 , integration is 10 ms. The scale bar is in the unit of counts per second. The pressure is 0.23 MPa, the temperature is $15.6 \text{ }^\circ\text{C}$; (b) and (c) are the bleaching time traces of two molecules in (a).

References:

1. Gaiduk, A.; Yorulmaz, M.; Orrit, M. *ChemPhysChem* **2011**, *12* (8), 1536-1541.
2. Cheng, Y.; Lu, G.; He, Y.; Shen, H.; Zhao, J.; Xia, K.; Gong, Q. *Nanoscale* **2016**, *8* (4), 2188-2194.
3. Onda, S.; Kobayashi, H.; Hatano, T.; Furumaki, S.; Habuchi, S.; Vacha, M. *J. Phys. Chem. Lett.* **2011**, *2* (21), 2827-2831.
4. Huser, T.; Yan, M.; Rothberg, L. J. *Proc. Natl. Acad. Sci. USA.* **2000**, *97* (21), 11187-11191.